REPORT DOCUMENTATION PAGE

Form Approved
OMB No. 0704-0188

1. REPORT DATE *(DD-MM-YYYY)*	**2. REPORT TYPE**	**3. DATES COVERED** *(From - To)*
14-09-2011	Journal Article	

4. TITLE AND SUBTITLE

Thermal Decomposition Mechanism of 1-ethyl-3methylimidzaolium bromide ionic liquid (Preprint)

5a. CONTRACT NUMBER

5b. GRANT NUMBER

5c. PROGRAM ELEMENT NUMBER

6. AUTHOR(S)
Steven D. Chambreau, Jerry A. Boatz, Ghanshyam L. Vaaghjiani, Christine Koh, Stephen R. Leone, Oleg Kostko, Amir Golan, and Daniel Strasser

5d. PROJECT NUMBER

5f. WORK UNIT NUMBER
23030423

7. PERFORMING ORGANIZATION NAME(S) AND ADDRESS(ES)

AFRL/RZSP
10 E. Saturn Blvd.
Edwards AFB, CA 93524-7680

8. PERFORMING ORGANIZATION REPORT NUMBER

AFRL-RZ-ED-JA-2011-377

9. SPONSORING / MONITORING AGENCY NAME(S) AND ADDRESS(ES)

Air Force Research Laboratory (AFMC)
AFRL/RZS
5 Pollux Drive
Edwards AFB CA 93524-7048

10. SPONSOR/MONITOR'S ACRONYM(S)

11. SPONSOR/MONITOR'S NUMBER(S)
AFRL-RZ-ED-JA-2011-377

12. DISTRIBUTION / AVAILABILITY STATEMENT

Approved for public release; distribution unlimited (PA #11836).

13. SUPPLEMENTARY NOTES
For publication in the JCP-A.

14. ABSTRACT

In order to better understand the volatilization process for ionic liquids, the vapor evolved from heating the ionic liquid 1-ethyl-3-methylimidazolium bromide was analyzed via tunable vacuum ultraviolet photoionization time of flight mass spectrometry (VUV-PI-TOFMS) and thermal gravimetric analysis mass spectrometry (TGA-MS). For this ionic liquid, the experimental results preclude the possible vaporization of intact ion-pairs or the formation of carbenes, but instead indicate the evolution of alkyl bromides and alkylimidazoles, presumably through alkyl abstraction via an SN2 type mechanism. Activation energies for the formation of the methyl and ethyl bromides were evaluated experimentally, and found to be in agreement with calculated values for the SN2 reactions. Comparisons of product photoionization efficiency (PIE) curves with literature data are in good agreement, and *ab initio* thermodynamics calculations are presented as further evidence for the proposed thermal decomposition mechanism. Estimates for the heat of vaporization of 1-ethyl-3-methylimidazolium bromide and 1-butyl-3- methylimidazolium bromide from molecular dynamics calculations and their gas phase heats of formation by G2MP2 calculations yield estimates for the ionic liquids' heats of formation in the liquid phase. .

15. SUBJECT TERMS

16. SECURITY CLASSIFICATION OF:			**17. LIMITATION OF ABSTRACT**	**18. NUMBER OF PAGES**	**19a. NAME OF RESPONSIBLE PERSON**
					Dr. Tommy W. Hawkins
a. REPORT	**b. ABSTRACT**	**c. THIS PAGE**	SAR	35	**19b. TELEPHONE NUMBER** *(include area code)*
Unclassified	**Unclassified**	**Unclassified**			N/A

Thermal decomposition mechanism of 1-ethyl-3-methylimidazolium bromide ionic liquid

Steven D. Chambreau,[1] Jerry A. Boatz,[2] Ghanshyam L. Vaghjiani[2,*]

Christine Koh,[3] Oleg Kostko,[4] Amir Golan,[4] Daniel Strasser,[5] Stephen R. Leone[3,4]

1. ERC, Inc., Edwards Air Force Base, California, 93524, U.S.A.
2. Propellants Branch, Propulsion Directorate, Air Force Research Laboratory, AFRL/RZSP, Edwards Air Force Base, California, 93524, U.S.A.
3. Departments of Chemistry and Physics, University of California, Berkeley, California, 94720, U.S.A.
4. Lawrence Berkeley National Laboratory, Berkeley, California, 94720, U.S.A.
5. Institute of Chemistry, Hebrew University, Jerusalem, 91904, Israel.

Abstract

In order to better understand the volatilization process for ionic liquids, the vapor evolved from heating the ionic liquid 1-ethyl-3-methylimidazolium bromide was analyzed via tunable vacuum ultraviolet photoionization time of flight mass spectrometry (VUV-PI-TOFMS) and thermal gravimetric analysis mass spectrometry (TGA-MS). For this ionic liquid, the experimental results preclude the possible vaporization of intact ion-pairs or the formation of carbenes, but instead indicate the evolution of alkyl bromides and alkylimidazoles, presumably through alkyl abstraction via an S_N2 type mechanism. Activation energies for the formation of the methyl and ethyl bromides were evaluated experimentally, and found to be in agreement with calculated values for the S_N2 reactions. Comparisons of product photoionization efficiency (PIE) curves with literature data are in good agreement, and *ab initio* thermodynamics calculations are presented as further evidence for the proposed thermal decomposition mechanism. Estimates for the heat of vaporization of 1-ethyl-3-methylimidazolium bromide and 1-butyl-3-methylimidazolium bromide from molecular dynamics calculations and their gas phase heats of formation by G2MP2 calculations yield estimates for the ionic liquids' heats of formation in the liquid phase.

* Email: ghanshyam.vaghjiani@edwards.af.mil; Tel: 661-275-5657; Fax: 661-275-5471

Keywords: ionic liquid, photoionization, thermal decomposition, photoionization efficiency, synchrotron

Introduction

Recent interest in ionic liquids, salts with melting points ≤ 100 °C, has stemmed from their extremely low volatility, thermal stability, and the enormous number of ionic liquids possible (~10^{18})[1] by varying either the cation or the anion. The physical and chemical properties of ionic liquids can also be tailored by modifying the functional groups on either ion. Ionic liquids have been studied for use as replacement solvents for volatile organic compounds (VOCs),[2-5] fuel cells,[6-9] electrolytes,[10,11] ingredients for energetic materials and propellants,[12-14] and as high temperature lubricants.[15-17]

Understanding thermal stability of ionic liquids is important for the safe storage and transportation of these compounds.[18] Protic ionic liquids, having a hydrogen bound to a nitrogen on the cation, have shown to be thermally unstable and easily neutralized via proton transfer to the anion.[19] These neutral species can volatilize and reform ionic liquids on co-condensation of the vapors by the acid-base reaction. Aprotic imidazolium ionic liquids, having alkylated nitrogens in the cation, have been seen to undergo dealkylation under pyrolytic conditions to yield 1-substituted imidazoles, presumably through an S_N2 type mechanism,[18,20-22] which would explain why the thermal stability of imidazolium-based ionic liquids increases with increasing anion size,[20,23] increasing the length of the side chain (steric effects),[20] or decreasing nucleophilicity of the anion.[20] Alkyl substituents such as vinyl and phenyl tend to increase the stability of the cation due to charge delocalization to the side chain and are not susceptible to cleavage,[20] while secondary and tertiary alkyl groups on the cation make the ionic liquid less thermally stable, presumably due to the elimination of the stabilized alkyl cations.[24] There also exists some evidence for the elimination of ethylene from ethylimidazolium ionic liquids with

increasing basicity of the anion.[20] The acidic character of the C2 proton of the imidazolium cation, illustrated by the facile deuterium exchange in D_2O,[25] seen also in thiazolium salts,[26] could also be a factor in the thermal stability of imidazolium-based ionic liquids, and addition reactions with the imidazolium ring have been observed at high temperatures.[22] Alkyl substitution of the C2 hydrogen on the imidazolium ring has the largest effect on the thermal stability due to the acidity of this proton.[24] This acidity stems from the stability of the carbene species formed upon proton loss from C2.[25,27] This n-heterocyclic carbene (NHC) species may play an important role in the addition reactions mentioned above,[28-30] and its formation can be facilitated by basic anions.[31] While the presence of oxygen does not appear to affect the temperature of decomposition of imidazolium ionic liquids, ionic liquids having endothermic decompositions in an inert atmosphere turn exothermic in an oxygen atmosphere midway through the observed mass loss in thermal gravimetric analysis (TGA) when combustion dominates.[24]

Previous studies on the vaporization of ionic liquids indicate that some aprotic ionic liquids, especially those with anions which are the conjugate bases of superacids,[32] vaporize as intact ion pairs, evidenced by the dissociative ionization of the ion pair and the detection of the intact cation by mass spectrometry: $C^+A^- + h\nu \rightarrow C^+A + e^- \rightarrow C^+ + A\bullet + e^-$. The removal of the electron from the anion eliminates the coulombic attraction between the ions, and the weakly bound cation-radical complex dissociates prior to detection in the mass spectrometer. Direct detection of the ion pair via mass spectrometric techniques has been elusive, but recent progress has been made to directly identify these in the gas phase.[33,34]

If the rates of thermal decomposition of ionic liquids are comparable to the rate of evaporation of ion pairs from the ionic liquid, the resulting species in the gas phase are a mixture

of thermal decomposition products and vaporized ion pairs. Effusive sources of ionic liquid vapors[35-38] impart substantial internal energy to the ion pair upon vaporization which can facilitate dissociation.

In this paper, a combination of mass spectrometric techniques is used to evaluate the gas phase decomposition products upon heating the aprotic ionic liquid 1-ethyl-3-methylimidazolium bromide ($EMIM^+Br^-$). The high sensitivity of vacuum ultraviolet photoionization time-of-flight mass spectrometry (VUV PI-TOFMS) enables the detection of thermal decomposition products well below the thermal decomposition onset temperature determined via differential scanning calorimetry (DSC) and thermal gravimetric analysis (TGA). The results from the TGA-MS experiments complement the VUV PI-TOFMS data and give a better understanding of the underlying processes and chemistry involved when heating $EMIM^+Br^-$. Accompanying *ab initio* calculations support the proposed decomposition mechanism by enabling the determination of possible photoion fragmentation pathways and gas phase heats of formation. The calculated gas phase heats of formation in conjunction with heats of vaporization determined by molecular dynamics simulations allow for estimation of heats of formation of ionic liquids in the liquid phase, a valuable but difficult to determine property of ionic liquids.

Experimental

Differential scanning calorimetry measurements were carried out with a typical sample mass of 5 mg at a heating rate of 2 K/min in sealed aluminum pans with a nitrogen flow rate of 20 ml/min (Figure 1). The reference sample was an empty Al container, which was sealed under nitrogen atmosphere.

Thermal gravimetric analysis mass spectrometry was carried out with electron impact ionization energy of 70 eV (Figure 2). An ionic liquid sample of approximately 5 mg was

analyzed under N_2 (10 ml/min) at 473 K for 1 hour, followed by increasing the temperature at a rate of 5 K/min up to 643 K. The capillary tube between the TGA unit and the mass spectrometer was held constant at 473 K.

The VUV-PI-TOFMS experiments were performed at the Chemical Dynamics beamline 9.0.2.3 at the Advanced Light Source synchrotron facility at the Lawrence Berkeley National Laboratory, Berkeley, CA. Details of the experiment and the effusive source have been described previously.[35,36] Briefly, photoionization mass spectra were measured from 8.0 to 15.0 eV in 0.2 eV steps at 457 K (Figure 3). At each energy the spectrum was averaged over 500,000 pulses of the ion repeller.

Ab initio calculations were carried out at the MP2/6-31+G(d,p) level of theory using GAMESS[39,40] and at the M06/6-31+G(d,p)[41] level of theory using Gaussian09[42]. All calculated results are at 0 K and include ZPVE corrections, unless otherwise stated. While B3LYP did not provide sufficient accuracy for these systems, MP2 and M06 methods provided accurate results when compared to similar bromine-containing species with known heats of formation. M06 resulted in comparable accuracy to MP2 for these systems with significantly reduced computational cost. Molecular dynamics (MD) simulations were performed using a polarizable force field, APPLE&P,[43] which was extended to include a description of the Br anion.

Results

Differential Scanning Calorimetry

In order to evaluate the thermal decomposition onset temperature for the ionic liquid in this study, differential scanning calorimetry (DSC) was carried out (Figure 1). For $EMIM^+Br^-$, the decomposition is exothermic, indicated by a positive peak. The jagged features in the DSC curve are as a result of the sealed aluminum sample holder bursting from the increase in pressure

upon decomposition. The onset thermal decomposition temperature, T_{dec}, for $EMIM^+Br^-$, reported as the initial nonzero slope of the DSC curves, is 585 K. It should be noted that for the VUV-PI-TOFMS experiments, temperatures well below this apparent onset decomposition temperature were chosen to look for possible vaporization of the ionic liquid (T=457, 510, 560 K).

Thermal Gravimetric Analysis: Mass Spectrometry

In an effort to understand the gas phase species evolved from the heated ionic liquid as a function of temperature, thermal gravimetric analysis mass spectrometry (TGA-MS) measurements were performed. Typical results for $EMIM^+Br^-$ are presented in Figure 2. In Figure 2a, the major product peaks detected are at masses 94($CH_3{}^{79}Br$), 96($CH_3{}^{81}Br$), 108($CH_3CH_2{}^{79}Br$), and 110($CH_3CH_2{}^{81}Br$), and their temperature profiles can be seen in Figure 2b. These masses are seen at all temperatures (473-643 K). Their relative mass intensities do not change significantly with increasing temperature, indicating that thermal decomposition occurs even at 473 K, which is well below the thermal decomposition onset temperature indicated in the DSC (T_{dec}=585 K, Figure 1).

VUV-PI-TOFMS

The mass spectra as a function of photon energy are shown in Figure 3 (T = 457 K), and the appearance energies (AE) of the photoions are presented in Table 1. No signals were detected which correspond to either the ion pair (masses 190 and 192 for $EMIM^+{}^{79}Br^-$ and $EMIM^+{}^{81}Br^-$, respectively) or the intact $EMIM^+$ cation (mass 111). Also absent from the mass spectra is mass 79, corresponding to $^{79}Br^+$. It should be noted that the $EMIM^+$ cation has been detected on the same apparatus under similar conditions previously with the ionic liquid 1-ethyl-3-methylimidazolium bistrifluorosulfonylamide.[38]

Discussion

Previous studies on aprotic imidazolium-based ionic liquids indicate their vaporization to intact C^+A^- ion pairs, based on the mass spectrometric detection of the intact cation, presumably following the dissociative ionization of the intact ion pair:

$$C^+A^- + h\nu \rightarrow C^+A + e^- \rightarrow C^+ + A\cdot + e^- \quad (1)$$

Even though the temperatures selected for the VUV PI-TOFMS experiments were well below the apparent onset decomposition temperature from the DSC (T_{dec}=585 K, Figure 1), a strong photoion signal was obtained in which signal corresponding to the cation resulting from the dissociative ionization of the ion pair ($EMIM^+$, mass 111) was noticeably absent. However, prominent peaks at 94, 96, 108 and 110 were observed. In order to determine if these peaks were as a result of dissociative photoionization of the $EMIM^+Br^-$ ion pair, *ab initio* calculations were performed at the MP2/6-31+G(d,p) level of theory to calculate the appearance energies in the photofragmentation of the anticipated ion pair (Figure 4). It was found that, within the expected uncertainties, these AEs are calculated to occur at approximately the same AE values that occur in the experiment. However, the MP2 calculated appearance energy for the EMIM cation at mass 111 is 6.8±0.1 eV (Figure 4) and mass 111 is not seen experimentally, which would preclude the presence of gaseous $EMIM^+Br^-$ ion pairs. Ultimately, by comparing not only the experimental appearance energies of the photoions to literature values of possible neutral species, but by also comparing their corresponding photoionization efficiency (PIE) curves to available literature PIE curves and photoelectron spectroscopy data, it is possible to identify the source of the photoions in our experiments. One beneficial aspect of the bromine system is that there are two isotopes of bromine: ^{79}Br and ^{81}Br, with natural isotope abundances of 50.69% and 49.31% respectively. The appearance of masses 108 and 110 with identical ion appearance

energies and PIE curve shapes, with a 1:1 ion signal ratio would indicate that these species have a bromine atom incorporated, and likely correspond to the $C_2H_5Br^+$ ion. When our low resolution PIE curves for masses 108 and 110 are compared to high resolution experimental total PIE data of ethyl bromide,[44] (Figure 5) not only are the photoion appearance energies equal (10.3 eV), but the features of the PIE curves match as well, strongly indicating that the photoion masses 108 and 110 originate due to the presence of ethyl bromide in the gas phase, and not from the dissociative photoionization of gaseous $EMIM^+Br^-$ ion pairs.

A similar analysis has been performed for the possibility of generating methyl bromide from the condensed phase heating of the $EMIM^+Br^-$ ionic liquid. In this case, the corresponding masses for $CH_3{}^{79,81}Br$ would be 94 and 96. However, in Figure 3 the signal from mass 96 is almost twice the intensity for mass 94, and this is likely due to the contribution from two different photoions to the mass 96 signal, $CH_3{}^{81}Br^+$ and the ethylimidazolium cation, the origin of which will be discussed below. These features are very similar to previous mass spectra generated by rapid thermolysis/mass spectrometric experiments on $EMIM^+Br^-$.[22] In comparison of the experimental PIE curve to the literature PIE of methyl bromide,[45] the appearance energies are equal (10.5 eV), the features of both curves match quite well (Figure 6a), and the derivative of the experimental PIE curve correlates with features in the literature photoelectron spectroscopy data[45] for CH_3Br (not shown). In addition, the PIE curves for the fragment ion, CH_2Br^+ (mass 93 and mass 95), have the same AEs (13.0 eV) and the curves match almost exactly (Figure 6b).

If methyl bromide and ethyl bromide are being formed by thermolysis in the heated ionic liquid, the condensed phase reactions involved would likely be:

$$EMIM^+Br^- \xrightarrow{\Delta} CH_3Br + EIM \qquad (2)$$

$$EMIM^+Br^- \xrightarrow{\Delta} CH_3CH_2Br + MIM \quad (3)$$

Where MIM is 1-methylimidazole (MW=82), and EIM is 1-ethylimidazole (MW=96). The measured AEs of photoion masses 82 (8.6 ± 0.2 eV) and 96 (8.5 ± 0.2 eV) match well with the MP2/6-31+G(d,p) calculated ionization potentials for MIM and EIM (8.66 ± 0.1 and 8.59 ± 0.1 eV), respectively, as well as with the NIST WEBBOOK[46] database value for MIM (8.66 eV). Assuming that the contribution from $CH_3{}^{81}Br$ to the mass 96 PIE curve is similar in strength to the PIE for $CH_3{}^{79}Br$, the experimental EIM^+ PIE curve can be obtained simply by subtracting the PIE of mass 94 ($CH_3{}^{79}Br$) from the observed PIE of mass 96 (Figure 7), resulting in an experimental ionization energy for EIM of 8.5 ± 0.2 eV. From the measured AE of mass 94 ($CH_3{}^{79}Br$), the AE of $CH_3{}^{81}Br$ of 10.5 ± 0.2 eV can be assumed (literature value for CH_3Br: IP = 10.54[47]).

The lower ion masses between 40-81 are dissociative fragments mainly of EIM with a small contribution from fragmentation of MIM, and their formation will be discussed below. Ion masses 26-30 are a combination of dissociative fragments from CH_3CH_2Br, MIM, and EIM, and their formation will not be discussed here. Mass 81 (AE = 11.1±0.2 eV) cannot be from $^{81}Br^+$, not only because there would be a comparable isotopic signal at mass 79 from $^{79}Br^+$, which is completely absent in Figure 3, but the $^{81}Br^+$ photoion appearance energy from CH_3Br is >15 eV.[45] Rather, the mass 81 peak could be from either dissociative photoionization of MIM or of EIM as follows:

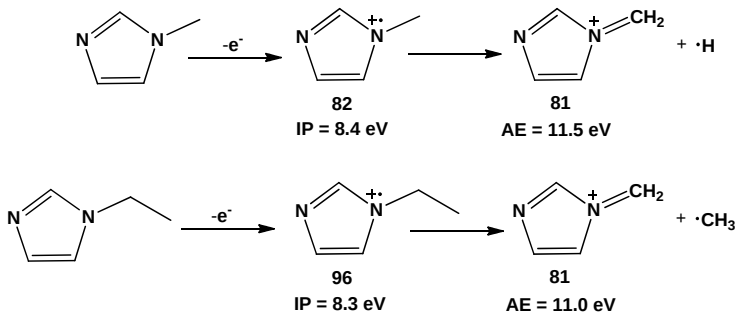

Scheme 1.

From the M06 calculated appearance energies for these two photofragments of 11.5±0.2 and 11.0±0.2 eV, respectively, the experimental appearance energy of 11.1±0.2 eV indicates that mass 81 more likely results from the latter fragmentation channel. The relative formation of $H^{79}Br$ (and the corresponding EMIM carbene, EMIM:) is negligible, as mass 80 is less than 1% of mass 82. This is consistent with calculations at the MP2/6-31+G(d,p) level, which show that (a) separated HBr + EMIM: is less stable than the $EMIM^+Br^-$ ion pair by 1.31 eV and (b) proton transfer from HBr to EMIM: to form the $EMIM^+Br^-$ ion pair occurs without an energy barrier. Mass 68 (AE = 10.9±0.2 eV) likely comes from EIM^+ fragmentation to form the imidazolium cation and the thermodynamically stable C_2H_4, a rather common ion fragmentation mechanism.[48] Although the calculated M06 energies (Scheme 2) for mass 68 ion formation do not match the experimental value exactly, the closest energy pathway is the hydrogen transfer from the ethyl CH_3 to C4 on the imidazolium ring, followed by elimination of C_2H_4 with a calculated AE = 11.5 eV.

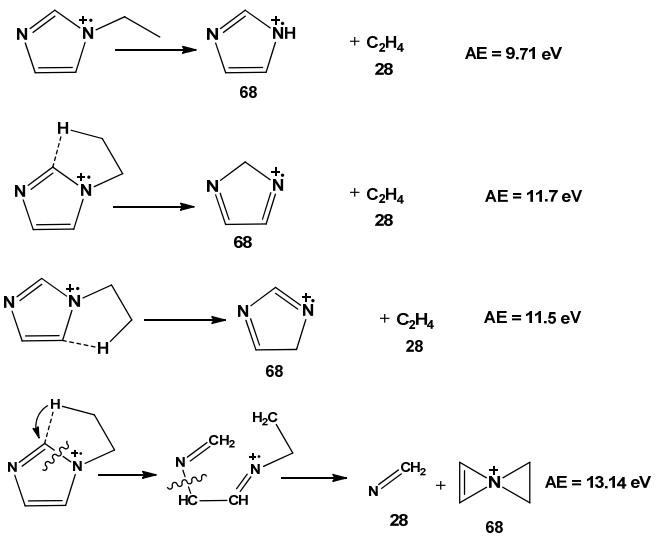

Scheme 2.

Another possibility is that the pathway leading to ethylene plus imidazolium ion via hydrogen transfer from the methyl group to N1 has a high barrier due to a strained geometry in the transition state, which could raise the AE above 9.74 eV. The pathway leading to formation of mass 68 ion plus CNH_2 was also considered, but the energetics are prohibitively high for this channel (AE = 13.1 eV, Scheme 2). The formation of mass 68 from MIM would involve the elimination of a CH_2 radical, which is highly energetically unfavorable (AE=13.2 eV):

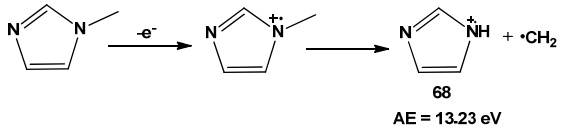

Also, from the literature, the electron impact ionization mass spectrum of EIM shows a mass 68 fragment whereas that of MIM does not, even at 70 eV ionization energy.[46]

Hydrogen transfer followed by ring opening fragmentation pathways will lead to masses 54(AE = 11.9±0.2 eV) and 42(AE = 12.0±0.2 eV). Ring opening without hydrogen transfer would lead to ion masses not observed in the experiment. While ring opening to form mass 54 can only occur from EIM, mass 42 can form from possible ring opening of both EIM and MIM.

To evaluate the fragmentation of EIM^+ (mass 96, $C_5N_2H_8$) to form mass 42 (C_2NH_4) and mass 54 (C_3NH_4), the heats of formation of the fragments with different possible structures, both neutrals and cations, were calculated at the M06/6-31+G(d,p) level of theory. The heats of formation of eight possible structures for mass 42 and 16 possible structures for mass 54 were evaluated, the appearance energies of each combination of cation and neutral fragments were calculated, and the fragmentation pathways within ±0.5 eV of the experimental AEs were evaluated further, resulting in nine pathways in this AE range for mass 54 cations and 26 pathways for mass 42 cations. From this analysis, the most likely pathways were determined (Scheme 3) by matching theoretical AEs to experimental AEs and looking for the most reasonable geometries resulting from fragmentation of EIM^+. Formation of the mass 42 and mass 54 fragments from the EIM^+ parent must involve a hydrogen transfer followed by two ring bond cleavages. The hydrogen transfer can come from the terminal methyl group on the ethyl to the C2 position on the imidazolium ring. The calculated M06 energies are in good agreement with the experimental AEs for this pathway. Mass 42 could possibly result from fragmentation of MIM to form mass 40 plus mass 42 (Scheme 3). However, the calculated AE for mass 42 is 12.7 eV, which doesn't match with the experimental mass 42 AE (11.9 eV) and the mass 40 signal is too small for this pathway to be significant.

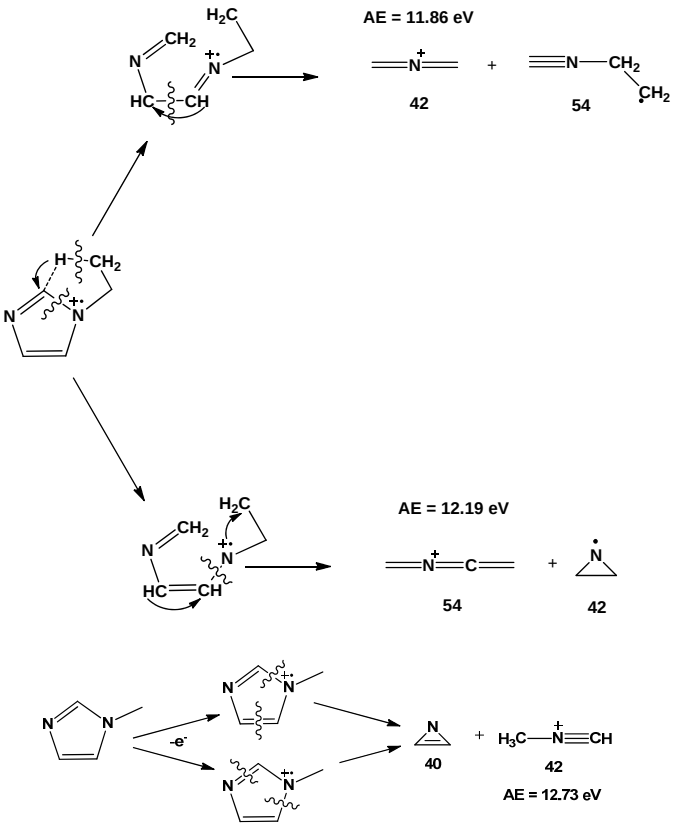

Scheme 3.

One possible source of ion mass 41 (AE = 12.7) would be from hydrogen transfer followed by ring cleavage of EIM to form masses 55 and 41. However, the mass 55 signal very small in this experiment, and this pathway has been ruled out. Instead, mass 41 could result from hydrogen transfer followed by ring cleavage to form two mass 41 fragments, and the calculated AE for the second pathway in Scheme 4 agrees very well with the experimental AE.

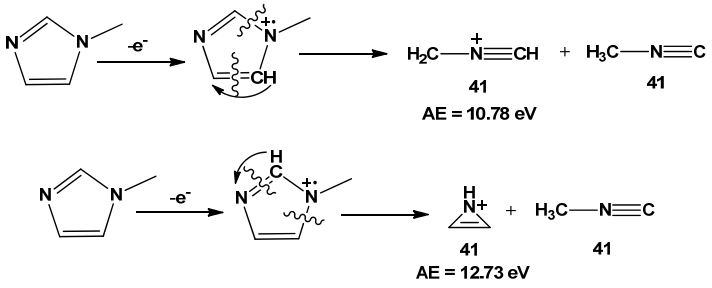

Scheme 4.

Assuming the rates of evaporation of CH_3Br (BP = 277 K,[46] ΔH^o_{vap} = 23.24 kJ/mol[46]) and CH_3CH_2Br (BP = 312 K,[46] ΔH^o_{vap} = 28.26 kJ/mol[46]) are much faster than the reaction rates of their formation at T = 454 K through reactions 2 and 3, the branching ratio between reactions 2 and 3 above can be calculated simply by comparing the ion counts (Figure 3) for methyl bromide versus ethyl bromide. To quantify the ethyl bromide reaction, the mass 108 and mass 110 photoion signals were summed over all photon energies and added together. To quantify the methyl bromide reaction, the mass 94 photoion signal was summed over all photon energies and multiplied by two in order to include the contribution from $CH_3{}^{81}Br$ (mass 96). At T = 454 K, the calculated branching ratio for CH_3Br: C_2H_5Br is 0.76:0.24.

Previous TGA-MS/DSC studies have suggested that significant mass loss can occur well below the thermal decomposition onset temperature.[18,49] In Figure 2b, the isothermal portion of the TGA curve at T=473 K indicates that >20% of the sample mass is lost in one hour, while the DSC does not indicate that any reaction takes place until almost 600 K. By making an Arrhenius plot with the natural log of the rate of product formation (ion signal intensity divided by temperature ramp rate, 5 K/min) versus 1/T (Figure 2c-d), the slope of the plot corresponds to $-E_a/R$ for the thermal decomposition. These activation barriers for masses 94, 96, 108 and 110 yield 112.1±6.6 kJ/mol and 118.4±7.2 kJ/mol for reactions 2 and 3 respectively, which are consistent with the VUV-PI-TOFMS branching ratio results reported above. Uncertainties in the experimental activation energies are the 95% confidence limits (±2σ, precision) determined by the linear least squares fit of the experimental data in figures 2c and 2d.

Ab initio calculations were performed to determine if the reaction proceeds via a bond insertion or via an S_N2 type mechanism. Transition states for Br^- to insert into the N-C bond of the methyl and ethyl side chains were located and their activation barriers were calculated. The

transition states were confirmed by frequency calculations resulting in a single imaginary frequency, and IRC calculations confirmed that the products were CH_3Br + EIM (reaction 2) or CH_3CH_2Br + MIM (reaction 3). The calculated activation barriers via bond insertion for reactions 2 and 3 are 239.3 kJ/mol and 212.1 kJ/mol, respectively (at M06/6-31+G(d,p) level of theory). Not only are these barriers prohibitively high, but also reaction 3 would be favored on energetic grounds, contrary to what is observed experimentally. However, for the S_N2 reactions, the transition state barriers and reaction enthalpies are in good agreement with experimental results. At the M06/6-31+G(d,p) level of theory, the activation energy (E_a) and heat of reaction (ΔH_{rxn}) are 133.1 kJ/mol and -85.8 kJ/mol, and 138.1 kJ/mol and 2.9 kJ/mol for reactions 2 and 3, respectively. The increased activation barrier for reaction 3 can be explained by steric factors, seen in Figure 8. The transition state for reaction 2 has a linear N-C-Br geometry with a near planar CH_3 group, and a C-Br distance of 2.55 Å at the M06/6-31+G(d,p) level of theory. The transition state for reaction 3 shows repulsion between the ethyl CH_3 group and the incoming Br^- which causes a bend in the N-C-Br angle away from linearity, and the C-Br distance elongates to 2.65 Å. Increasing the basis set to aug-cc-pvtz only decreases the C-Br distance by 0.02 Å to 2.63 Å, therefore the moderate size of the 6-31+G(d,p) basis set is appropriate to accurately describe the transition state geometry for reaction 3. The decrease in magnitude of E_a values from theory to experiment is likely due to solvent stabilization effects in the condensed phase relative to the gas phase, where the ionic liquid solvent lowers the energy of the transition state more than it does for the reactant.

To determine whether vaporization competes with thermal decomposition under vacuum distillation conditions, it is necessary to estimate the heat of vaporization for $EMIM^+Br^-$. In order to estimate the heat of vaporization of $EMIM^+Br^-$, several approaches were investigated.

Recent work by Paulechka and coworkers[50] on the thermochemistry of the formation of 1-butyl-3-methylimidazolium bromide ($BMIM^+Br^-$) determined that the heat of vaporization of $BMIM^+Br^-$ is sufficiently higher than the activation barrier for thermal decomposition such that saturated vapor pressure due to intact $BMIM^+Br^-$ will never be experimentally attainable. Although the heat of formation of halogen containing compounds can be calculated from the heat of combustion, experimental determinations of heats of combustion of halogen containing compounds are difficult to determine accurately due to incomplete combustion and the need to accurately identify combustion products. Instead, Paulechka measured the heat of reaction $MIM_{(l)} + BuBr_{(l)} \rightarrow BMIM^+Br^-_{(l)}$ calorimetrically, where BuBr is 1-butylbromide, and calculated the heat of formation of the ionic liquid from this measurement using known C_p values and heats of formation of MIM and BuBr. By adding the experimentally determined activation energy to the heat of the reaction for: $MIM_{(l)} + BuBr_{(l)} \rightarrow BMIM^+Br^-_{(l)}$, the activation energy for the reverse reaction (thermal decomposition) can be calculated (Figure 9). With an activation energy of E_a = 73±4 kJ/mol (determined over the range of 303-334 K) and ΔH_{rxn} (298 K) = 87.7±1.6 kJ/mol, the resulting activation barrier for the reverse reaction is 161±4 kJ/mol. From the experimentally determined heat of formation of $BMIM^+Br^-_{(l)}$ as well as the gas phase heat of formation of the ion pair calculated by quantum chemical methods, the heat of vaporization was determined to be ΔH_{vap} (298 K) = 174 ± 9 kJ/mol. Since the estimated ΔH_{vap} (298 K) = 174±9 kJ/mol is greater than the barrier for the reverse reaction (161±4 kJ/mol), on energetics grounds, thermal decomposition will dominate, and vaporization to ion pairs will not be experimentally detectable.

An alternate method for determining the heat of formation in the liquid phase of the ionic liquid is to calculate the heat of formation of the ion pair in the gas phase by *ab initio* methods

(G2MP2), and to calculate the heat of vaporization of the ionic liquid using molecular dynamics (MD) methods. If the heat of formation of the gaseous ion pair and the heat of vaporization can be calculated, the heat of formation in the liquid phase of the ionic liquid can be calculated as the difference between the gas phase heat of formation and the heat of vaporization (see Figure 9). The gas phase heats of formation $\Delta H_{f,\,gas}$(298 K) of $EMIM^+Br^-$ and $BMIM^+Br^-$ at the G2(MP2) level of theory are 32.2±20 and -11.7±20 kJ/mol, and the $\Delta H_{f,\,gas}$(298 K) value for $BMIM^+Br^-$ agrees within error limits with the literature value of $\Delta H_{f,\,gas}$(298 K) = 16±7 kJ/mol.[50] The uncertainty of the G2(MP2) calculations for systems involving bromine were estimated at ±20 kJ/mol by comparing calculated G2(MP2) heats of formation of bromine containing molecules to their known literature values (Table 3). The difference in the gas phase heats of formation $\Delta H_{f,\,gas}$(298 K) between $EMIM^+Br^-$ and $BMIM^+Br^-$ of 43.9 kJ/mol is consistent with the general trend of decreasing $\Delta H_{f,\,gas}$(298 K) from C_2MIM to C_4MIM observed recently.[51] Using the value of 32.2±20 kJ/mol for the G2MP2 gas phase heat of formation of $EMIM^+Br^-$ and, at first approximation, assuming the heat of vaporization of $EMIM^+Br^-$ is the same as that of $BMIM^+Br^-$ (174±9 kJ/mol), the heat of formation of $EMIM^+Br^-_{(l)}$ is calculated to be -142±22 kJ/mol at 298 K. To improve on the accuracy of this value, molecular dynamics simulations were carried out to determine the heat of vaporization (ΔH_{vap}) of $EMIM^+Br^-$ (Table 2).[52] Heats of vaporization at 298 K were determined for $EMIM^+Br^-$ and $BMIM^+Br^-$ by extrapolation from the heats of vaporization determined by molecular dynamics simulations at higher temperatures as indicated in Table 2. Molecular dynamics simulations were performed for both $EMIM^+Br^-$ and $BMIM^+Br^-$ in order to validate the ΔH_{vap} with Paulechka's experimental value for $BMIM^+Br^-$. Comparison of the ΔH_{vap}(298 K) value for $BMIM^+Br^-$ from Table 2 (152.8 kJ/mol) with the ΔH_{vap}(298 K) from Paulechka and coworkers (174 kJ/mol) indicates the molecular dynamics value is low by

~14%. Correcting for this observed systematic error would yield an estimate for $EMIM^+Br^-$ ΔH_{vap}(298 K) of 169±25 kJ/mol. Using this value and the G2MP2 gas phase heat of formation of $EMIM^+Br^-$, our best estimate for the heat of formation of $EMIM^+Br^-_{(l)}$ is -136±25 kJ/mol at 298 K. A corresponding result for $BMIM^+Br^-_{(l)}$ yields a ΔH_f value of -186±25 kJ/mol, which is consistent, within reported uncertainties, with that of Paulechka (-158±5 kJ/mol). Similar to the findings for $BMIM^+Br^-$,[50] the ΔH_{vap} value for $EMIM^+Br^-$ at 473 K of 130.8 kJ/mol is significantly larger than the experimental E_a values for thermal decomposition (112.1 and 118.4 kJ/mol for reactions 2 and 3) that saturated vapor pressure of $EMIM^+Br^-$ is unattainable, and thermal decomposition effectively dominates the mass loss process for $EMIM^+Br^-$ in our experiments.

Conclusion

The absence of mass 111 ($EMIM^+$ cation) from the effusive source VUV-PI-TOFMS experiments preclude the possibility of vaporization of $EMIM^+Br^-$ as intact ion pairs. Instead, the observed photoions and PIE curves strongly indicate the decomposition of $EMIM^+Br^-$ to CH_3Br, CH_3CH_2Br, MIM and EIM. TGA-MS studies and *ab initio* calculations support the S_N2 mechanism whereby CH_3Br formation is favored 3 to 1 over CH_3CH_2Br formation due to increased steric hindrance in the transition state for the latter path. From this work, the best estimates for the heat of formation and the heat of vaporization of $EMIM^+Br^-$ are ΔH_f(298 K)=-136±25 kJ/mol and ΔH_{vap}(298 K)=169±25 kJ/mol.

Acknowledgements

Funding for this work was provided by the Air Force Office of Scientific Research under contract No. FA9300-06-C-0023 with the Air Force Research Laboratory, Edwards AFB, CA

93524. We would like to thank Erik Mitchell for obtaining the DSC data, Greg Yandek and Ray Campos for the TGA data, and Wasatch Molecular Inc. for the molecular dynamics ΔH_{vap} data. This work was supported in part by a grant of computer time from the DoD High Performance Computing Modernization Program at the Air Force Research Laboratory, Army Research Laboratory, Engineer Research and Development Center, and Navy Department of Defense Supercomputing Resource Centers (DSRCs).

Table 1. VUV photoion appearance energies (in eV, ±0.2 eV) for the gaseous products when 1-ethyl-3-methylimidazolium bromide is heated to 457 K.

Mass	**41**	**42**	**54**	**68**	**81**	**82**	**94**	**96**	**108**	**110**
Appearance Energy	12.7	12.0	11.9	10.9	11.1	8.6	10.5	8.5	10.3	10.3

Table 2. Heats of vaporization determined by molecular dynamics simulations.[52]

Heat of vaporization.	T (K)	ΔH_{vap} (kJ/mol)
$EMIM^+Br^-$	298	147.1[b]
$EMIM^+Br^-$	393	138.3[a]
$EMIM^+Br^-$	473	130.8[a]
$BMIM^+Br^-$	298	152.8[b]
$BMIM^+Br^-$	323	150.5[a]
$BMIM^+Br^-$	393	144.0[a]

[a]MD direct calculation
[b]linear extrapolation from higher temperature MD values

Table 3. Error analysis of G2(MP2) method for bromine-containing systems. Energies are in kJ/mol.

	$\Delta H_{f,gas}$ G2(MP2)	experiment	Error
Br^-	-227.4	-212.7	14.7
HBr	-49.7	-36.3	13.4
CH_3Br	-48.7	-34.3	14.6
CH_3CH_2Br	-75.3	-63.6	11.7

Captions

Figure 1. Differential scanning calorimetry (DSC) curve for 1-ethyl-3-methylimidazolium bromide ionic liquid (solid line). Dotted line is the slope of the DSC curve. T_{dec} = 585 K.

Figure 2(a) TGA-MS data of $EMIM^+Br^-$ averaged over 60 minutes at 473 K. (b) TGA-MS data of $EMIM^+Br^-$ and for masses 94, 96, 108, and 110 as a function of temperature. The isotherm at 473 K is represented by the vertical dashed line. (c) Arrhenius plot for determination of E_a for the formation of CH_3Br. (d) Arrhenius plot for determination of E_a for the formation of C_2H_5Br.

Figure 3. VUV PI-TOFMS results for heated $EMIM^+Br^-$ ionic liquid in an effusive source, with source temperature T=457 K. Photoion appearance energies are listed in Table 1.

Figure 4. Energetics of the possible dissociative photoionization of $EMIM^+Br^-$. Stationary points are calculated at the MP2/6-31+G(d,p) level of theory (0 K, ZPVE corrected).

Figure 5. Photoionization efficiency (PIE) curves for mass 108 ($C_2H_5{}^{79}Br^+$) and mass 110 ($C_2H_5{}^{81}Br^+$). Solid curve is total PIE data for C_2H_5Br from reference 44 (reproduced with permission of The Royal Society of Chemistry).

Figure 6(a) Experimental PIE data for mass 94 ($CH_3{}^{79}Br^+$) and (b) experimental PIE curve for mass 93 ($CH_2{}^{79}Br^+$). Solid curves are total PIE data for CH_3Br from reference 45 (reproduced with permission from Elsevier).

Figure 7. PIE curves for mass 94 and mass 96. Triangles are the difference of mass 96 and mass 94 PIE curves, and represents the PIE curve for EIM^+.

Figure 8. Transition states for the S_N2 alkyl abstraction of methyl (top) and ethyl (bottom) by the bromide ion at the M06/6-31+G(d,p) level of theory.

Figure 9. Energy diagram for the conversion of $BMIM^+Br^-$ to MIM + BuBr (data used with permission from reference[50]).

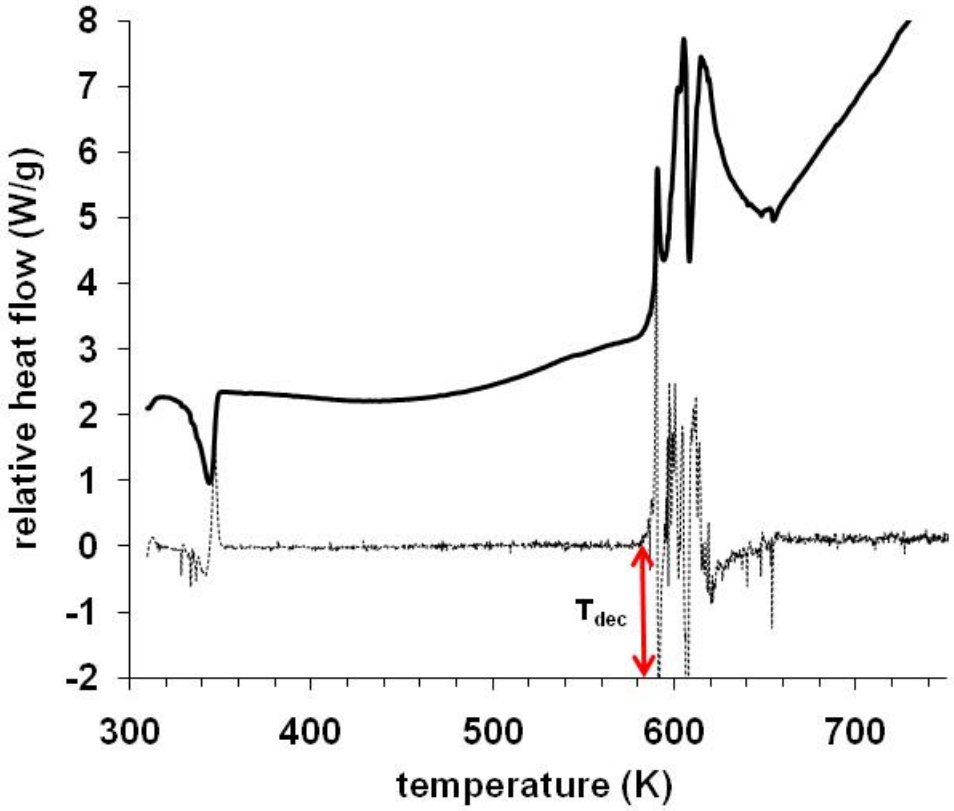
relative heat flow (W/g)
8
7
6
5
4
3
2
1
0
-1
-2
300
400
500
600
700
temperature (K)
T dec

Figure 1.

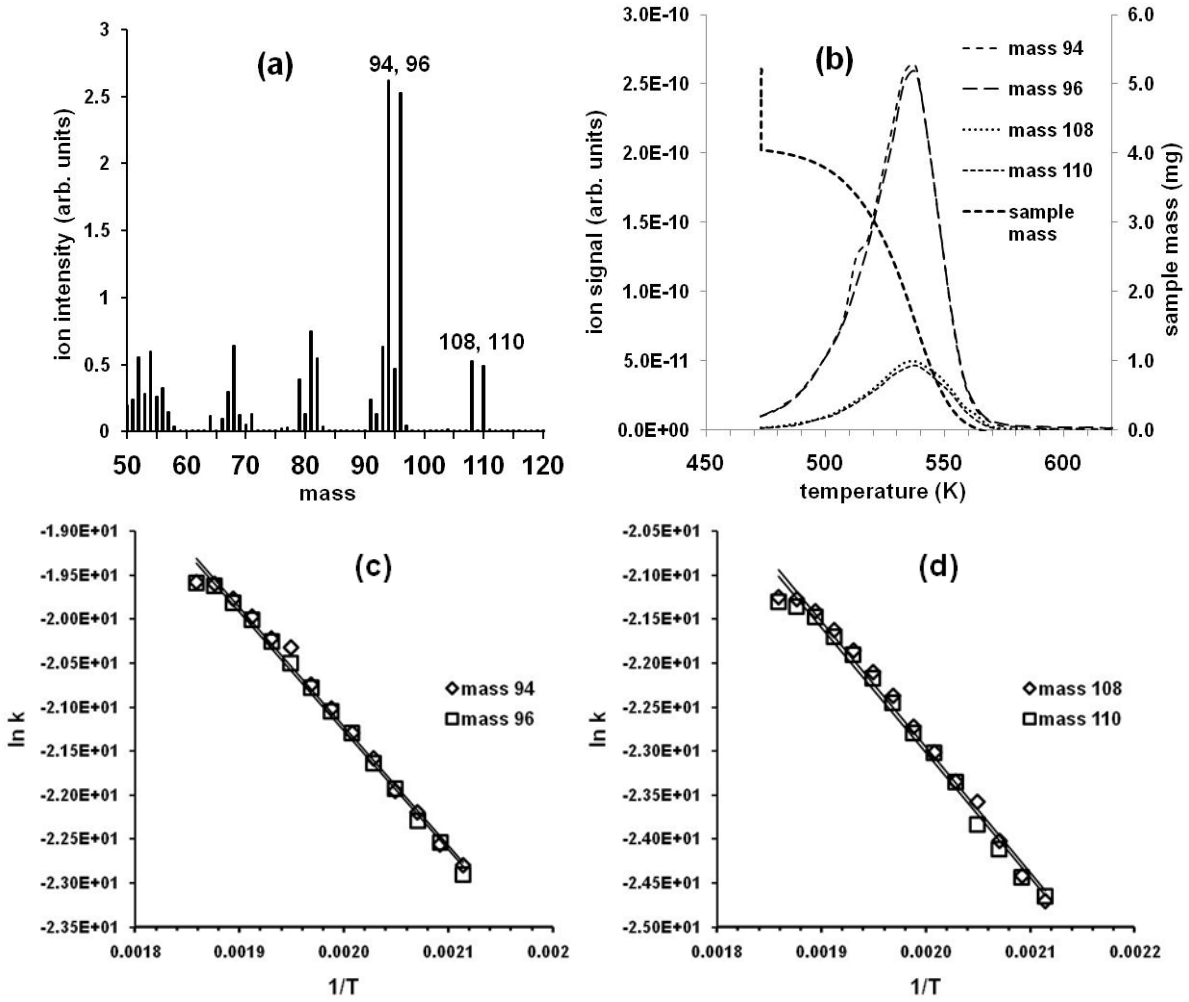
(a)
94, 96
108, 110
ion intensity (arb. units)
mass
(b)
mass 94
mass 96
mass 108
mass 110
sample mass
ion signal (arb. units)
sample mass (mg)
temperature (K)
(c)
mass 94
mass 96
ln k
1/T
(d)
mass 108
mass 110
ln k
1/T

Figure 2a-d.

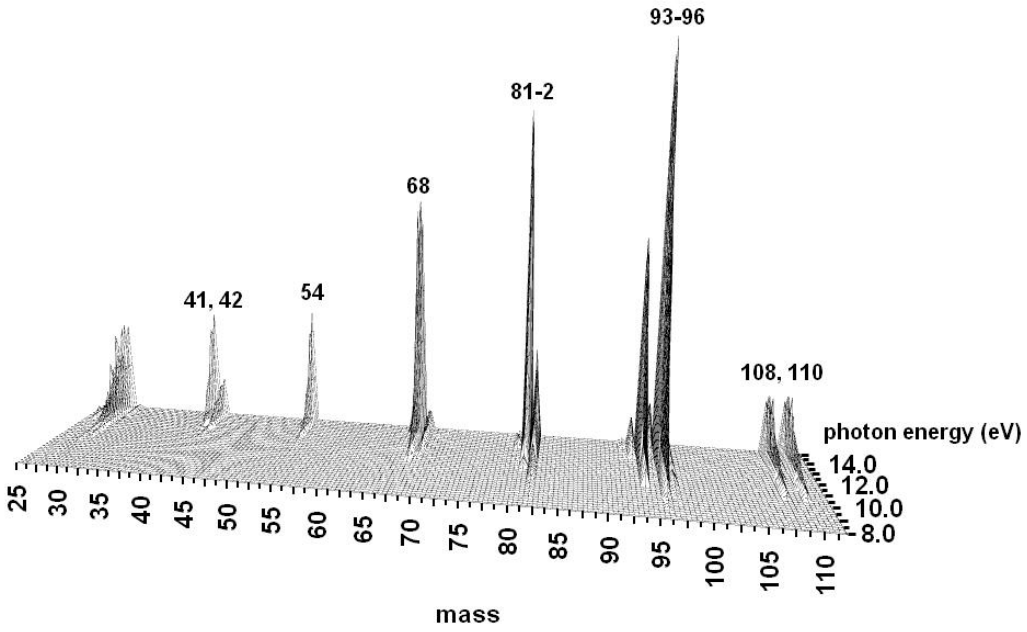
93-96
81-2
68
54
41, 42
108, 110
photon energy (eV)
14.0
12.0
10.0
8.0
25
30
35
40
45
50
55
60
65
70
75
80
85
90
95
100
105
110
mass

Figure 3.

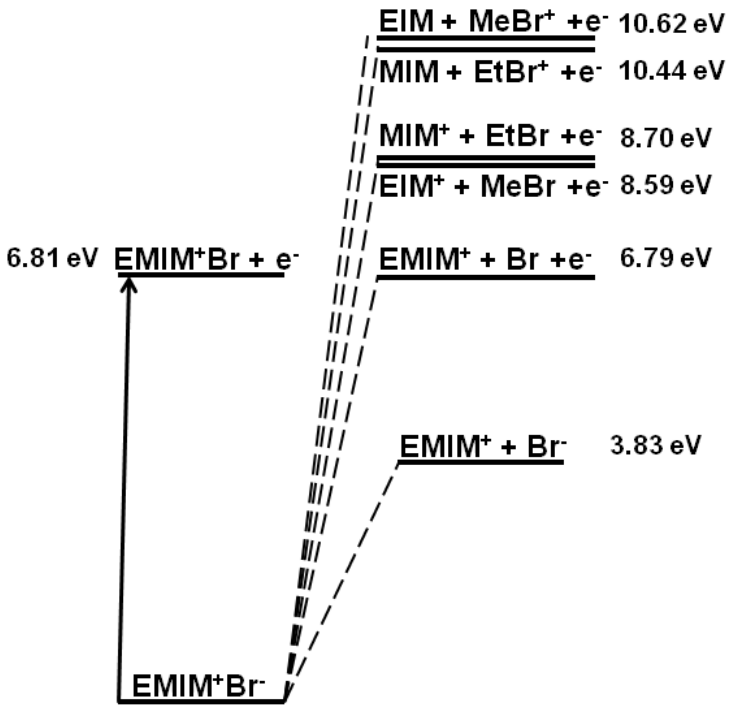
EIM + MeBr+ +e- 10.62 eV
MIM + EtBr+ +e- 10.44 eV
MIM+ + EtBr +e- 8.70 eV
EIM+ + MeBr +e- 8.59 eV
6.81 eV EMIM+Br + e-
EMIM+ + Br +e- 6.79 eV
EMIM+ + Br- 3.83 eV
EMIM+Br-

Figure 4

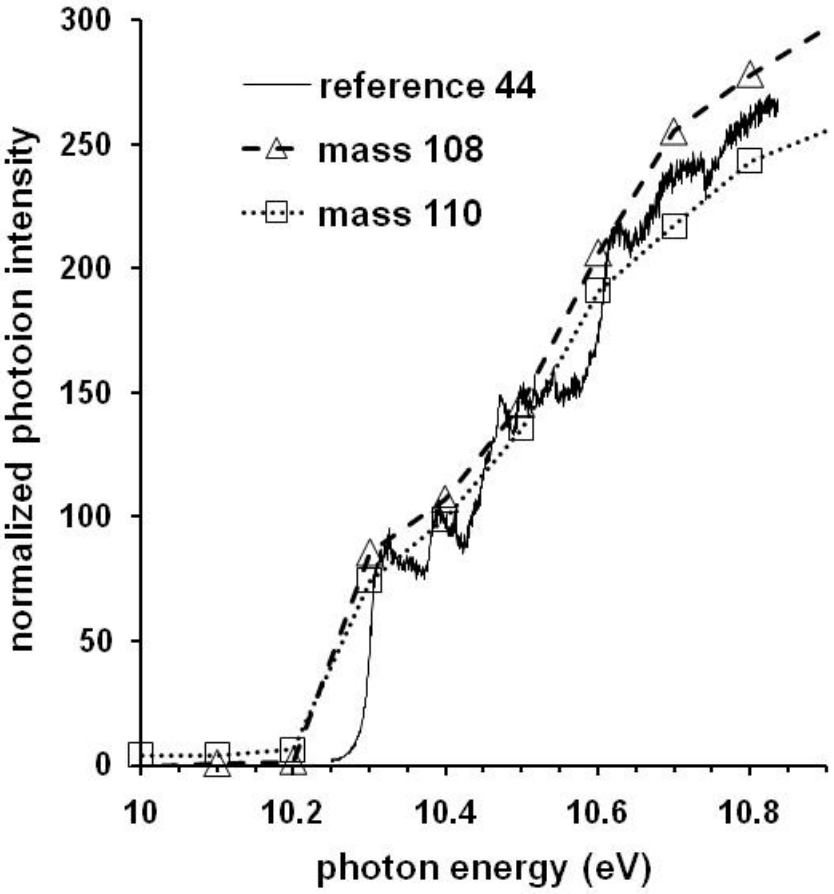
300
250
200
150
100
50
0
normalized photoion intensity
reference 44
mass 108
mass 110
10
10.2
10.4
10.6
10.8
photon energy (eV)

Figure 5.

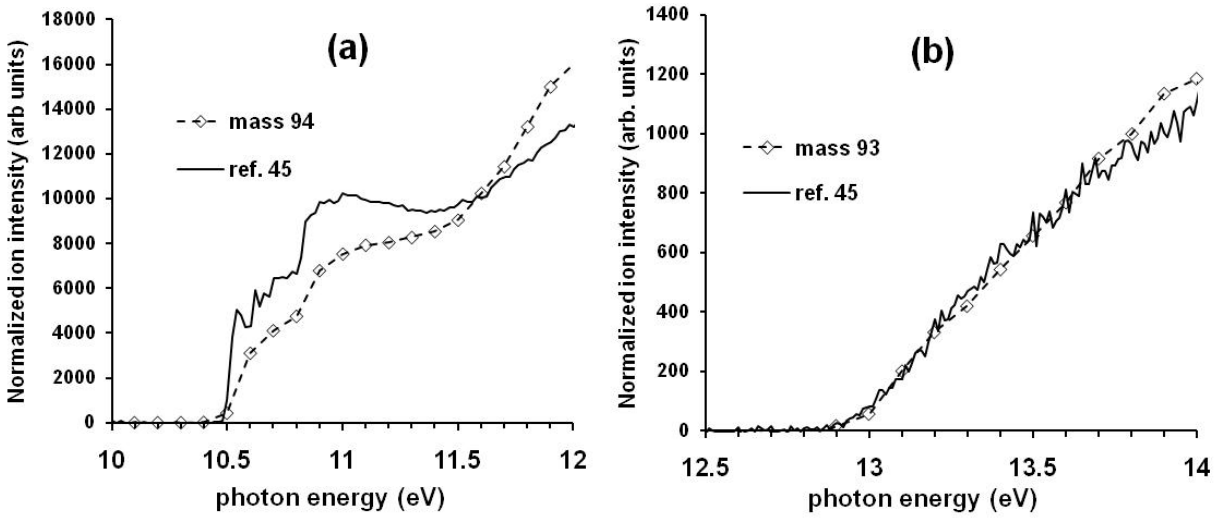
(a)
mass 94
ref. 45
Normalized ion intensity (arb units)
photon energy (eV)
(b)
mass 93
ref. 45
Normalized ion intensity (arb. units)
photon energy (eV)

Figure 6a-b.

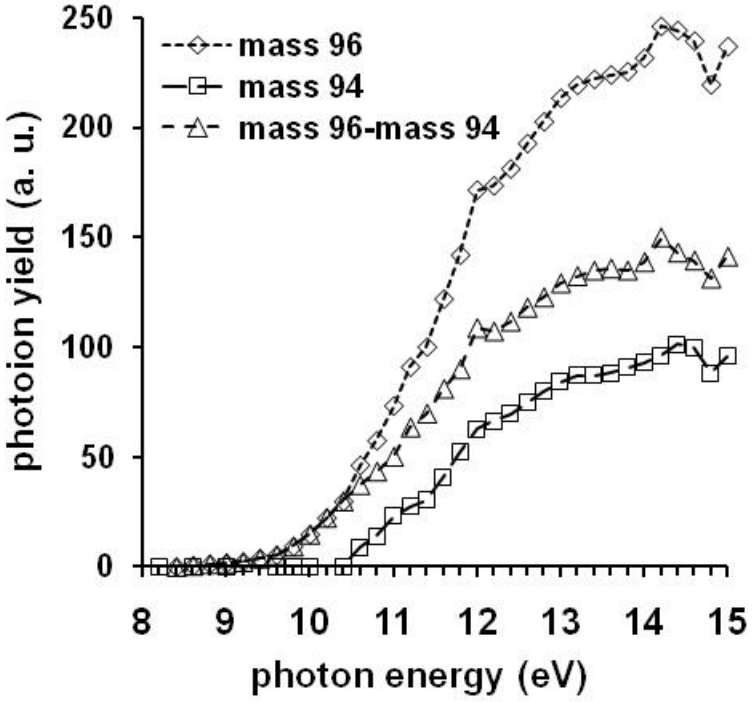
250
200
150
100
50
0
photoion yield (a. u.)
mass 96
mass 94
mass 96-mass 94
8
9
10
11
12
13
14
15
photon energy (eV)

Figure 7.

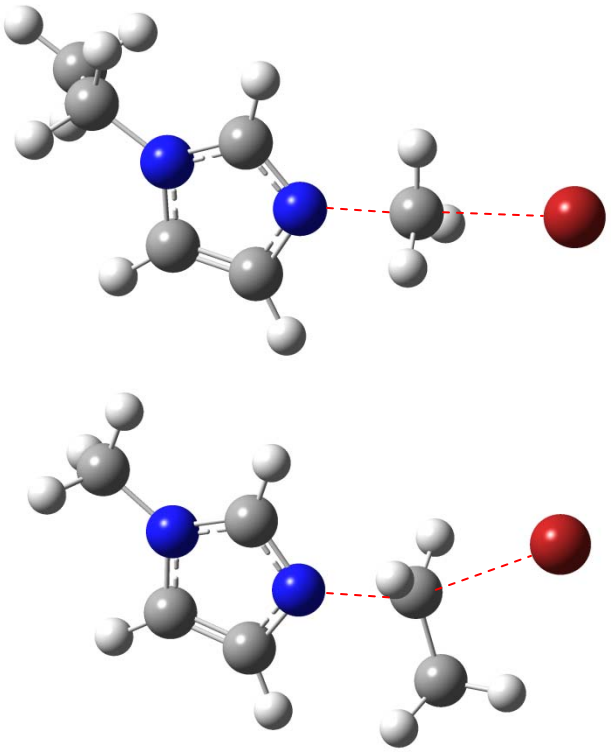

Figure 8.

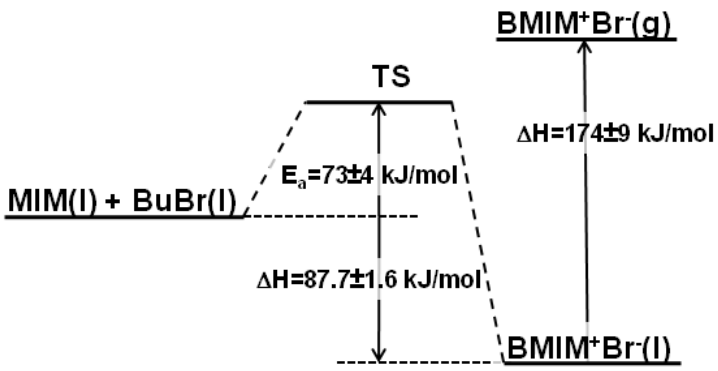
BMIM+Br-(g)
TS
ΔH=174±9 kJ/mol
Ea=73±4 kJ/mol
MIM(l) + BuBr(l)
ΔH=87.7±1.6 kJ/mol
BMIM+Br-(l)

Figure 9.

REFERENCES

(1) Plechkova, N. V.; Seddon, K. R. Applications of ionic liquids in the chemical industry *Chem. Soc. Rev.* **2008**, *37*, 123-150.

(2) Friere, M. G.; Neves, C. M. S. S.; Marrucho, I. M.; Canongia Lopes, J. N.; Rebelo, L. P. N.; Coutinho, J. A. P. High-performance extraction of alkaloids using aqueous two-phase systems with ionic liquids *Green Chem.* **2010**, *12*, 1715-1718.

(3) Giunta, D.; Solinas, M. Beneficial Combination of Ionic Liquids and Carbon Dioxide in Transition Metal Catalysed Reactions *Curr. Org. Chem.* **2009**, *13*, 1300-1321.

(4) Sheldon, R. Catalytic reactions in ionic liquids *Chem. Commun.* **2001**, *23*, 2399-2407.

(5) Visser, A. E.; Swatloski, R. P.; Griffin, S. T.; Hartman, D. H.; Rogers, R. Liquid/liquid extraction of metal ions in room temperature ionic liquids *Separation Sci. Technol.* **2001**, *36*, 785-804.

(6) Di Noto, V.; Negro, E.; Sanchez, J.-Y.; Lojoiu, C. Structure-Relaxation Interplay of a New Nanostructured Membranew Based on TetraethylammoniumTrifluoromentanesulfonate Ionic Liquid and Neutralized Nafion 117 for High-Temperature Fuel Cells *J. Am. Chem. Soc.* **2010**, *132*, 2183-2195.

(7) Kim, S. Y.; Kim, S.; Park, M. J. Enhanced Proton Transport in Nanostructured Polymer Electrolyte/ionic Liquid Membranes Under Water-Free Conditions *Nature Communications* **2010**, *1*

(8) Nakamoto, H.; Noda, A.; Hayamizu, K.; Hayashi, S.; Hamaguchi, H.; Watanabe, M. Proton-Conductiong Properties of Bronsted Acid-Base Ionic Liquid and Ionic Melts Consisting of Bis(trifluoromethanesulfonyl)imide and Benzimidazole for Fuel Cell Electrolytes. *J. Phys. Chem. C* **2007**, *111*, 1541-1548.

(9) Yasuda, T.; Ogawa, A.; MKanno, M.; Mori, K.; Sakakibara, K.; Watanabe, M. Hydrophobic Protic Ionic Liquid for Nonhumidified Intermediate-Temperature Fuel Cells *Chem. Lett.* **2009**, *38*, 692-693.

(10) Armand, M.; Endres, F.; MacFarlane, D. R.; Ohno, H.; Scrosati, B. Ionic-Liquid Materials for the Electrochemical Challenges of the Future *Nature Mater.* **2009**, *8*, 621-629.

(11) Zakeeruddin, S. M.; Graetzel, M. Solvent-Free Ionic Liquid Electrolytes for Mesoscopic Dye-Senstitzed Solar Cells *Adv. Func. Mater.* **2009**, *19*, 2187-2202.

(12) Chambreau, S. D.; Schneider, S.; Rosander, M.; Hawkins, T.; Gallegos, C. J.; Pastewait, M. F.; Vaghjiani, G. L. Fourier Transform Infrared Studies in Hypergolic Ignition of Ionic Liquids *J. Phys. Chem. A* **2008**, *112*, 7816-7824.

(13) Gao, H.; Joo, Y.-H.; Twamley, B.; Zhou, Z.; Shreeve, J. n. M. Hypergolic Ionic Liquids with the 2,2-Dialkyltriazinium Cation *Angew. Chem. Int. Ed.* **2009**, *48*, 2792-2795.

(14) Hawkins, T.; Rosander, M.; Vaghjiani, G. L.; Chambreau, S. D.; Drake, G.; Schneider, S. Ionic Liquids as Hypergolic Fuels *Energy Fuels* **2008**, *22*, 2871-2872.

(15) Bermudez, M.-D.; Jimenez, A.-E.; Sanes, J.; Carrion, F.-J. Ionic liquids as advanced lubricant fluids *Molecules* **2009**, *14*, 2888-2908.

(16) Palacio, M.; Brushan, B. A Review of Ionic Liquids for Green Molecular Lubrication in Nanotechnology *Tribol. Lett.* **2010**, *40*, 247-268.

(17) Van Renesselar, J. Unleashing the potential of ionic liquids *Tribol. Lubricat. Technol.* **2010**, *66*, 24-31.

(18) Baranyai, K. J.; Deacon, G. B.; MacFarlane, D. R.; Pringle, J. M.; Scott, J. L. Thermal Degradation of Ionic Liquids at Elevated Temperatures *Aust J Chem* **2004**, *57*, 145-147.

(19) Leal, J. P.; Esperança, J. M. S. S.; Minas da Piedade, M. E.; Canongia Lopes, J. N.; Rebelo, L. P. N.; Seddon, K. R. The Nature of Ionic Liquids in the Gas Phase *J. Phys. Chem. A* **2007**, *111*, 6176-6182.

(20) Chan, B. K. M.; Chang, N.-H.; Grimmett, M. R. The Synthesis and Thermolysis of Imidazole Quaternary Salts *Aust J Chem* **1977**, *30*, 2005-2013.

(21) Kroon, M. C.; Buijs, W.; Peters, C. J.; Witkamp, G.-J. Quantum chemical aided prediction of the thermal decomposition mechanisms and temperatures of ionic liquids *Thermochim. Acta* **2007**, *465*, 40-47.

(22) Chowdhury, A.; Thynell, S. T. Confined rapid thermolysis/FTIR/ToF studies of imidazolium-based ionic liquids *Thermochim. Acta* **2006**, *443*, 159-172.

(23) Fredlake, C. P.; Crosthwaite, J. M.; Hert, D. G.; Aki, S. N. V. K.; Brennecke, J. F. Thermophysical Properties of Imidazolium-Based Ionic Liquids *J. Chem. Eng. Data* **2004**, *49*, 954-964.

(24) Ngo, H. L.; LeCompte, K.; Hargens, L.; McEwen, A. B. Thermal Properties of Imidazolium Ionic Liquids *Thermochim. Acta* **2000**, *357-358*, 97-102.

(25) Handy, S. T.; Okello, M. The 2-position of Imidazolium Ionic Liquids: Substitution and Exchange *J. Org. Chem.* **2005**, *70*, 1915-1918.

(26) Breslow, R. Rapid Deuterium Exchange in Thiazolium Salts *J. Am. Chem. Soc.* **1957**, *79*, 1962-1963.

(27) Arduengo, A. J.; Harlow, R. L.; Kline, M. A Stable Crystalline Carbene *J. Am. Chem. Soc.* **1991**, *113*, 361-363.

(28) Breslow, R. Mechanism of Thiamine Action: Participation of a Thiazolium Zwitterion *Chemistry and Industry* **1957**, *26*, 893-894.

(29) Wanzlick, H. W.; Schonherr, H. J. Chemistry of Nucleophilic Carbenes. XVIII. 1,3,4,5-Tetraphenylimidazolium Perchlorate *Liebigs Ann. Chem.* **1970**, *731*, 176.

(30) Kan, H.-C.; Tseng, M.-C.; Chu, Y.-H. Bicyclic imidazolium-based ionic liquids: synthesis and characterization *Tetrahedron* **2007**, *63*, 1644-1653.

(31) Holloczki, O.; Gerhard, D.; Massone, K.; Szarvas, L.; Nemeth, B.; Veszpremi, T.; Nyulaszi, L. Carbenes in Ionic Liquids *New Journal of Chemistry* **2010**, *34*, 3004-3009.

(32) Koppel, I. A.; Taft, R. W.; Anvia, F.; Hu, L.-Q.; Sung, K.-S.; DesMarteau, D. D.; Yagupolskii, L. M.; Yagupolskii, Y. L.; Ignat'ev, N. V.; Kondratenko, N. V., et al. The Gas-Phase Acidities of Very Strong Neutral Bronstead Acids *J. Am. Chem. Soc.* **1994**, *116*, 3047-3057.

(33) Gross, J. H. Molecular Ions of Ionic Liquids in the Gas Phase *J. Am. Soc. Mass Spectrom.* **2008**, *19*, 1347-1352.

(34) Chambreau, S. D.; Vaghjiani, G. L.; Koh, C.; Golan, A.; Strasser, D.; Leone, S. R. Photoionization Efficiency of 1-Butyl-3-Methylimidazolium Tricyanomethanide Ionic Liquid Vapors **in preparation**

(35) Chambreau, S. D.; Vaghjiani, G. L.; To, A.; Koh, C.; Strasser, D.; Kostko, O.; Leone, S. R. Heats of Vaporization of Room Temperature Ionic Liquids by Tunable Vacuum Ultraviolet Photoionization *J. Phys. Chem. B* **2010**, *114*, 1361-1367.

(36) Strasser, D.; Goulay, F.; Belau, L.; Kostko, O.; Koh, C.; Chambreau, S. D.; Vaghjiani, G. L.; Ahmed, M.; Leone, S. R. Tunable Wavelength Soft Photoionization of Ionic Liquid Vapors *J. Phys. Chem. A* **2010**, *114*, 879-883.

(37) Strasser, D.; Goulay, F.; Kelkar, M. S.; Maginn, E. J.; Leone, S. R. Photoelectron Spectrum of Isolated Ion-Pairs in Ionic Liquid Vapor *J. Phys. Chem. A* **2007**, *111*, 3191-3915.

(38) Koh, C.; Liu, C.-L.; Harmon, C.; Strasser, D.; Golan, A.; Kostko, O.; Chambreau, S. D.; Vaghjiani, G. L.; Leone, S. R. Soft ionization of thermally evaporated hypergolic ionic liquid aerosols *J. Phys. Chem. A* **2011**, *115*, 4630-4635.

(39) Gordon, M. S.; Schmidt, M. W. Advances in Electronic Structure Theory: GAMESS a Decade Later. In *Theory and Applications of Computational Chemistry: the First Forty Years*; Dykstra, C. E., Frenking, G., Kim, K. S., Scuseria, G. E., Eds.; Elsevier: Amsterdam, 2005; pp 1167-1189.

(40) Schmidt, M. W.; Baldridge, K. K.; Boatz, J. A.; Elbert, S. T.; Gordon, M. S.; Jensen, J. H.; Koseki, S.; Matsunaga, N.; Nguyen, K. A.; Su, S., et al. General Atomic and Molecular Electronic Structure System *J. Comput. Chem.* **1993**, *14*, 1347-1363.

(41) Zhao, Y.; Truhlar, D. G. The M06 suite of density functionals for main group thermochemistry, thermochemical kinetics, noncovalent interactions, excited states, and transition elements: two new functionals and systematic testing of four M06-class functionals and 12 other functionals *Theor. Chem. Account.* **2008**, *120*, 215-241.

(42) Frisch, M. J.; Trucks, G. W.; Schlegel, H. B.; Scuseria, G. E.; Robb, M. A.; Cheeseman, J. R.; Scalmani, G.; Barone, V.; Mennucci, B.; Petersson, G. A., et al. "Gaussian 09, Revision A.02," Gaussian, Inc., 2009.

(43) Borodin, O.; Smith, G. D.; Kim, H. Viscosity of a Room Temperature Ionic Liquid: Predictions from Nonequilibrium and Equilibrium Molecular Dynamics Simulations *J. Phys. Chem. B* **2009**, *113*, 4771-4774.

(44) Baer, T.; Song, Y.; Liu, J.; Chen, W.; Ng, C. Y. Pulsed field ionization-photoelectron photoion coincidence spectroscopy with synchrotron radiation: The heat of formation of the $C_2H_5^+$ ion *Faraday Discuss.* **2000**, *115*, 137-145.

(45) Locht, R.; Leyh, B.; Dahareng, D.; Hottmann, K.; Jochims, H. W.; Baumgartel, H. About the photoionization of methyl Bromide (CH_3Br). Photoelectron and photoionization mass spectrometric investigation *Chem. Phys.* **2006**, *323*, 458-472.

(46) Afeefy, H. Y.; Liebman, J. F.; Stein, S. E. Neutral Thermochemical Data. In *NIST Chemistry WebBook, NIST Standard Reference Database Number 69*; Linstrom, P. J., Mallard, W. G., Eds.; National Institute of Standards and Technology.

(47) Lias, S. G. Ionization Energy Evaluation. In *NIST Chemistry WebBook, NIST Standard Reference Database Number 69*; Linstrom, P. J., Mallard, W. G., Eds.; National Institute of Standards and Technology.

(48) Yamaoka, H.; Fokkens, R. H.; Nibbering, N. M. M. A metastable ion and collision-induced dissociation study of the (M-C2H4)-+ ion from 3-phenyl-1-bromopropane *Int. J. Mass. Spectrom.* **1999**, *188*, 1-6.

(49) Arellano, I. H. J.; Guarino, J. G.; Paredes, F. U.; Arco, S. D. Thermal Stability and Moisture Uptake of 1-Alkyl-3methylimidazolium Bromide *J. Therm. Anal. Calorim.* **2011**, *103*, 725-730.

(50) Paulechka, Y. U.; Kabo, A. G.; Blokhin, A. V. Calorimetric Determination of the Enthalpy of 1-butyl-3-methylimidazolium Bromide Synthesis: A Key Quantity in Thermodynamics of Ionic Liquids *J. Phys. Chem. B* **2009**, *113*, 14742-14746.

(51) Fumino, K.; Wulf, A.; Verevkin, S. P.; Heintz, A.; Ludwig, R. Estimating Enthalpies of Vaporization of Imidazolium-Based Ionic Liquids from Far-Infrared Measurements *ChemPhysChem* **2010**, *11*, 1623-1626.

(52) Bedrov, D.; Hooper, J. B., Wasach Molecuar, Inc., Molecular Dynamics Determination of ΔH_{vap} of Imidazolium Bromide Ionic Liquids, private communication.